ELSEVIER

Sedimentary Geology 148 (2002) 389–403

Sedimentary Geology

www.elsevier.com/locate/sedgeo

A lowstand epikarstic intertidal flat from the middle Silurian of Gotland, Sweden

Mikael Calner *

Department of Geology, Division of Historical Geology, Lund University, Sölvegatan 13, SE-223 62 Lund, Sweden

Received 17 August 2000; accepted 29 June 2001

Abstract

This paper describes the sedimentology, morphology and diagenesis of recently discovered Middle Silurian low-relief micro-epikarst from the Klintehamn area on western Gotland (Sweden). The epikarst represents the most distal portion of an unconformity that truncates stratigraphic units across a major part of the Baltic palaeo-basin. It formed in the intertidal area during the late stage of platform development and following a short period of regression and siliciclastic influx to the basin at the closing of the *Cyrtograptus lundgreni* Chron. An overlying oncolite shows signs of repeated exposure to meteoric and marine waters, supporting the interpretation of a karstic flat setting. Four microfacies with different stable isotopic signatures are recognised across the unconformity: *dolomitic siltstone* and *altered siltstone* in the topmost Fröjel Formation, below the contact, and *ferruginous crinoid algal packstone* and *ferruginous oncolite grainstone* above the contact, in the basal lag of the transgressive Halla Formation. Endolithic structures of inferred fungal/algal origin occur frequently in the two transgressive microfacies. The set of observations pointing towards subaerial exposure and karstic processes include: (a) an understanding of the regional geology; (b) erosional relief with undercutting and an associated conglomerate; (c) vertical and subvertical conduits (karren), indicating gravitationally controlled waters; (d) widening of fissures and subsequent polyphase fillings (splitkarren); (e) eluviated, internal sediment (e.g., crystal silt); (f) blackening; (g) repeated etching of carbonate allochems; (h) a fitted grain-fabric; (i) circum-granular cracking; (j) pendant nonluminescent cements; (k) abundant intercrystalline and intergranular (secondary) porosity, and (l) anomalous stable isotopes. A synsedimentary iron-crust at the contact was not related to karstification but formed a few centimetres below the sediment surface during the ensuing transgression.

Keywords: Epikarst; Gotland; Silurian; Stable isotopes

1. Introduction

Recognition of ancient karst is critical to our understanding of past evolution of carbonate platforms and climate (e.g., Esteban and Klappa, 1983; Choquette and James, 1988). However, careful microfacies analysis is necessary if features inherited from subaerial and submarine dissolution should be separated unequivocally (a good example from the Jurassic Tethys realm was discussed by Di Stefano and Mindszenty, 2000). Silurian karst has earlier been described in detail from relatively few areas, but with

* Fax: +46-46-12-14-77.
E-mail address: Mikael.Calner@geol.lu.se (M. Calner).

0037-0738/02/$ - see front matter
PII: S0037-0738(01)00144-0

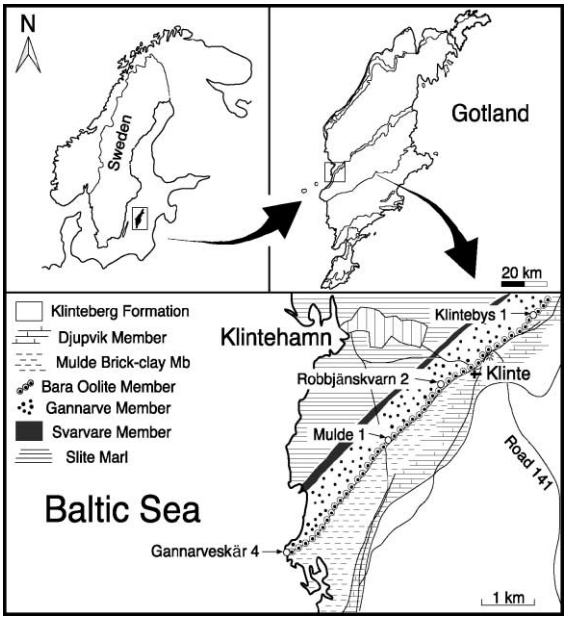

Fig. 1. The mid-late Homerian outcropbelt and the discussed localities in the Klintehamn area of western Gotland. Terminology after Calner (2000).

notably good descriptions from the Llandovery Byron and Manistique dolomites of Wisconsin and the Kankakee Dolomite of Illinois (Kluessendorf and Mikulic, 1996), the Wenlock Lockport and Peebles Dolomites of Ohio (Kahle, 1988), and from the Ludlow Eke Formation of Gotland (Cherns, 1982). Herein I add a recently discovered karstic flat and rocky shore to the knowledge of Silurian karst. It forms the unconformable boundary between the regressive Gannarve Member of the Fröjel Formation and the transgressive Bara Oolite Member of the Halla Formation on western Gotland (Fig. 1). Additional data regarding these units and related localities are given by Calner (1999) and Calner and Säll (1999).

2. Background

The first published lines about the unconformity described herein were by Munthe (1915, p. 431), who noted its presence at the Klintebys 1 locality (Fig. 1). He recognised an erosional relief of a few centimetres on the top of the underlying siltstone (now referred to as the Gannarve Member) and the presence of rounded siltstone pebbles–gravels in the lowermost part of the oolite (Munthe, 1915). When Hede later mapped the bedrock geology in the area, he traced the oolite southwestwards to Robbjänskvarn 2 and Mulde 1, however, without providing any rigorous description of the unconformity (Hede, 1921, 1927, summarised 1960). Instead, he largely quoted the results of Munthe but added that the unconformable boundary also could be seen ca. 1000 m to the west, as well as ca. 1000 m to the northeast of Klintebys 1 (Hede, 1927, p. 32–33; these places are now cultivated areas without outcrops). He also added that a ca. 1-mm-thin crust of iron oxide (limonite) in places covered the unconformity. Unfortunately, he did not mention at what localities, but these are likely to be among the two new localities he reported, and hence, the iron-crust may cover many thousands of square metres. Hadding, in his survey of Palaeozoic and Mesozoic sandstones of Sweden, considered the Gannarve Member only briefly (Hadding, 1929, p. 184; the 'Slite Sandstone'). His study was petrographic and Munthe (1915) was quoted about the unconformity. More recent workers in this stratigraphic interval have traditionally quoted Hede (e.g., Sivhed, 1976) who in turn largely quoted from the brief investigation of Munthe (1915). Accordingly, until today no attention has fallen on this unconformity, and the first picture of the distinct contact was published almost 90 years after its discovery (Calner, 1999, fig. 5d). Although the unconformity long has been regarded as a local feature, recent work has revealed also its regional and global significance (Calner, 2000); sequence- and biostratigraphical analysis has showed that the uneven surface at Klintebys 1 represents the most distal portion of an unconformity that truncates stratigraphic units across a major part of the Baltic palaeo-basin (Fig. 2) and that it locally yields at least 16 m of palaeotopography (Calner and Säll, 1999). Eventstratigraphic analysis has further demonstrated the relationship of the unconformity and the global extinctions among, e.g., conodonts, chitinozoans and graptolites at the closing of the *Cyrtograptus lundgreni* Chron (Jaeger, 1991; Koren', 1991; Kaljo et al. 1995; Jeppsson, 1997, 1998; papers in Calner, 2000). The present study aims to reconstruct the micro-stratigraphy and the sequence

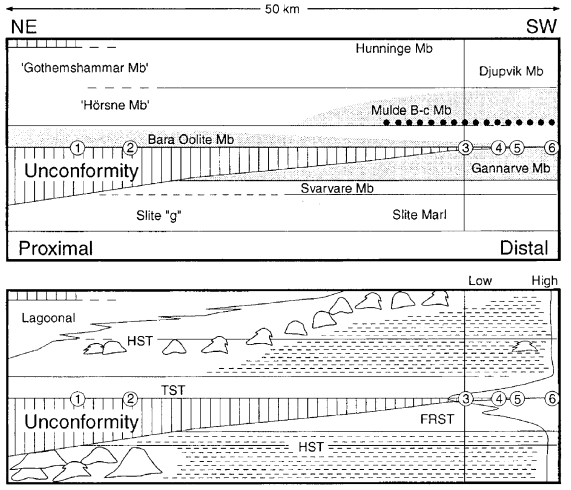

Fig. 2. Schematic lithostratigraphy (upper) and an inferred sequence stratigraphic model (lower) for the uppermost Slite Group (below the unconformity), the Halla Formation, and the lowermost part of the Klinteberg Formation (Hunninge Member). In the upper drawing, the shaded areas indicate the relative condensation (thickening/thinning) trends of specific members. Note that due to erosional diachroni along the unconformity, the transgressive systems tract (TST) rests on the preceding highstand systems tract (HST) on the proximal platform, but on the forced regressive systems tract (FRST) along the platform palaeomargin (the vertical line marks the shoreline position during the closing of the *C. lundgreni* Chron). Black dots represent the stratigraphic position of the Grötlingbo Bentonite. Numbers refer to localities along the unconformity: 1 = Svalings 1, 2 = Bara 1, 3 = Klintebys 1, 4 = Robbjänskvarn 2, 5 = Mulde 1, 6 = Gannarveskär. See Calner et al. (2000) for details of the reef distribution, and Calner (2000) for biostratigraphic ties to the sea-level curve.

of changes across the contact in order to delineate its origin and genesis.

3. Material and methods

The material for this study comes from Klintebys 1 (the major part), Mulde 1 and Gannarveskär 4 (detailed in Figs. 2 and 3). At Klintebys 1, only limited horizontal surfaces are available for study and observations are mainly made from vertical faces. A selection of polished slabs and explanatory sketches are shown in Figs. 4 and 5. Observations are listed in descending order, roughly after scale: the most obvious and those seen in outcrop and on hand-specimens first, and those that require good magnification, last. Individual beds at Klintebys 1 are referred to by their sample numbers (given in Fig. 3). The data set for the study includes many tens of polished slabs from which 21 were selected for making thin sections. Thin sections were studied by means of a standard petrographic microscope, cathodoluminescence (CL) microscopy and through element detection analysis (EDX). Seven additional whole-rock samples for study under scanning electron microscope (SEM) were cut perpendicular or horizontal to bedding, and were subsequently polished and etched for 20 s in 0.1 M hydrochloric acid. Measurements of insoluble content were based on 20 g samples of homogenised material. The samples were crushed and dissolved in hydrochloric acid before the insoluble residue was weighed. Reference materials are housed at the Department of Geology, Division of Historical Geology and Palaeontology, Lund University.

4. Relief and morphology of the epikarst

The unconformity truncates a tangentially cross-laminated, dolomitic siltstone bed, with a preserved thickness maximum of ca. 5 cm (Figs. 4 and 5). The bed is frequently penetrated and a wide variety of solution features, typically associated to karst (e.g., Choquette and James, 1988; Kahle, 1988), occur to at least 10–15 cm below the contact. The surface of truncation is *not* bored or mineralised, but shows spots of blackening and etching. The topography is variably sharp-edged to smooth showing different types of down-cutting morphologies (karren) separated by longitudinal ridges and knobs. These are mostly close to vertical or display varying degree of undercut, and may rarely be lined by a dense and structureless, grey coating, inferably of algal origin. Karren morphology varies from channels, to broad depressions with irregular bottoms (kamenitzas), and to wedge-shapes (grikes). Oval, sub-circular to circular micro-swallets (sinkholes), penetrating the first bed under the contact (bed 423), are common and generally 10–15 mm in diameter. They are well separated laterally and do not form ‘swiss-cheese’ channel boxworks (Baceta et al., in press). Their orientation varies from vertical to subhorizontal. Cavities protruding upward, a few millimetres into the lower bedding plane of bed 423, are common. Vertical calcite-filled fractures are frequent,

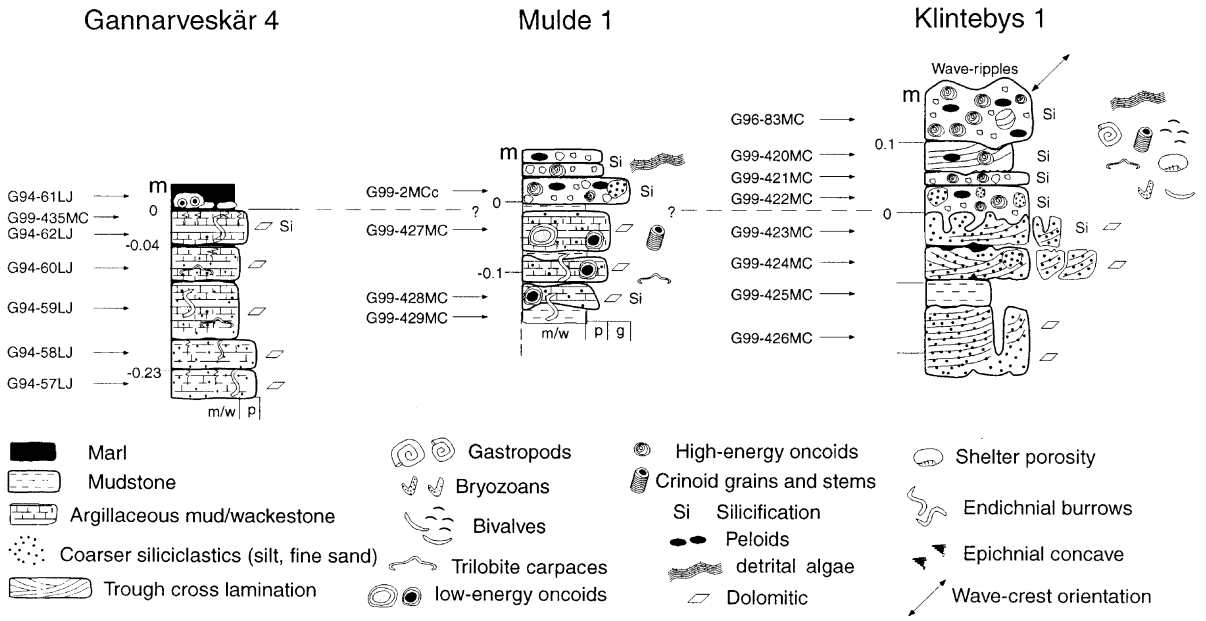

Fig. 3. Sedimentary profiles of the Gannarve and Bara Oolite members at localities which palaeogeographically were distributed along the transition from the platform interior to the seaward platform slope (see also Calner et al., 2000).

originating both from the upper and lower boundaries of bed 423, indicating some mechanical compaction following the lithification of the Gannarve Member (Figs. 4c–d and 5d).

The truncated surface is partly covered by a 1–3 mm thin, dark reddish crust of limonite (Hede, 1927; Calner, 1999). In contrast to earlier studies (Hede, 1927; Sivhed, 1976), the samples collected for this study show that iron not only occurs as a crust, but also is confined to a 10–30-mm-thick zone. A geopetal origin for the zone is clearly shown by its relative stratigraphic position to the karst morphology and microfacies, e.g., the absence of the crust at arches and in troughs outside the vertical range of the zone (Figs. 4 and 5), its 'hanging' position below clasts (Fig. 4a), and in particular in its lateral extent into the topmost Gannarve Member and the basal Bara Oolite Member (Fig. 5b). In the Gannarve Member, iron is irregularly distributed in the intergranular are, visible as black, sand-sized spots on polished slabs (e.g., Fig. 5c–d). In the Bara Oolite Member, the iron is concentrated in the cortex of coated grains. The iron crust itself is only an expression for the lithological differences where the zone crosses microfacies boundaries. Several minute iron-stained surfaces ('satellite crusts'), truncating allochems and cements, occur above this crust, in the lowermost centimetres of the Bara Oolite Member.

5. Microfacies descriptions

Four microfacies occur in association to the unconformity. *Dolomitic siltstone* and *altered siltstone* occur below the contact, forming the topmost Gannarve Member, and represent the unaffected and affected parent rock, respectively. *Ferruginous crinoid algal packstone* and *ferruginous oncolitic grainstone* occur above the contact, representing a condensed transgressive lag facies belonging to the basal Bara Oolite Member. The total thickness of the four microfacies varies from a few to less than 10 cm. In addition, a siltstone conglomerate is associated to the succession of microfacies.

5.1. Dolomitic siltstone (DS)

The topmost Gannarve Member shows great variation in composition, from sandstone with carbonate matrix (rare) to dolomitic and silty, poorly fossilifer-

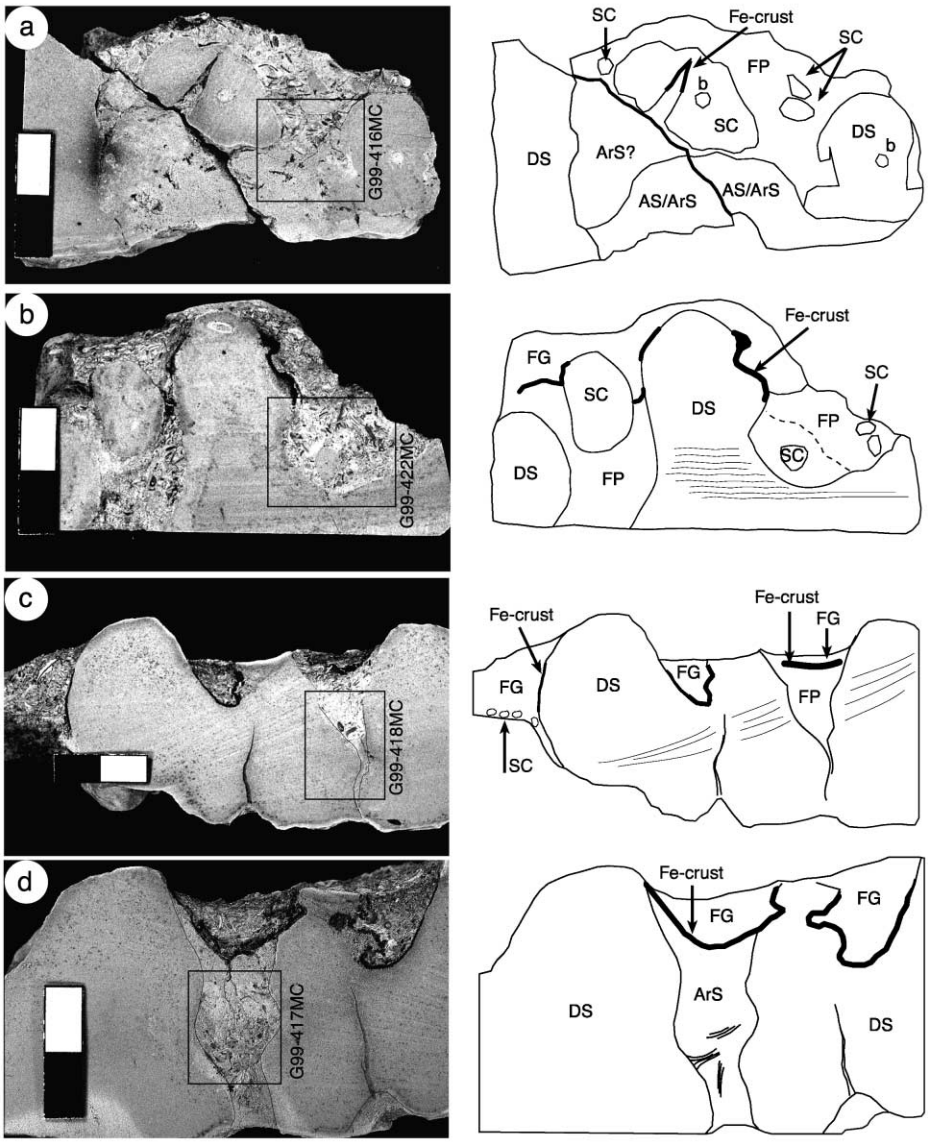

Fig. 4. Epikarst morphology and microfacies distribution at Klintebys 1. Squares and associated numbers mark position of thin-sections referred to in the text and in the reference material. Scale-bar = 2 cm. Note that thin lines have been added in figure (c) and (d) to enhance the morphology of karren. (a) Typical vertical down-cuttings and gravel-sized siltstone clasts (SC). Note borings (indicated with 'b') in both SC and DS microfacies. (b) Smooth topography with slight undercut in laminated siltstone. Note well-developed iron-crust that separates the FP and FG microfacies. (c) Sharp-edged topography with wedge-shaped karren (grike) to the right. The iron-crust separates the FG and FP microfacies, the latter with the cream-white matrix variety. AS microfacies occur in the lowermost part of the grike, below FP. Note calcite vein originating from small cavity on the lower bedding plane. (d) Micro-swallet with infill of ArS and FG separated by the iron-crust. The ArS microfacies contain abundant calcite laths. Note calcite vein originating from small cavity on the lower bedding plane.

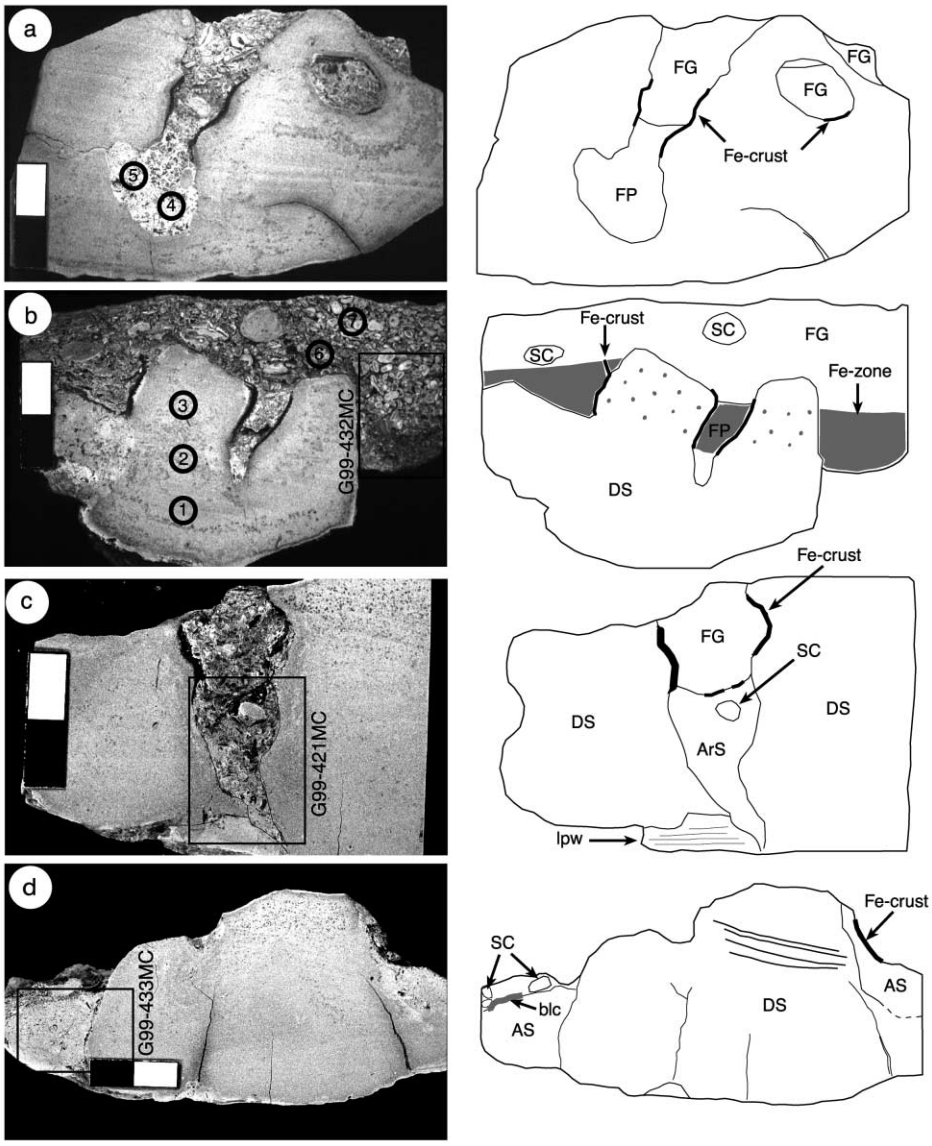

Fig. 5. Epikarst morphology and microfacies distribution at Klintebys 1. Squares and associated numbers mark position of thin-sections referred to in the text. Scale-bar = 2 cm. Note that thin lines have been added in figure (c) to enhance the morphology of karren. (a) Two stages of channel development. Presence of FP facies in the left channel indicates that it never penetrated the bed. The channel to the right was sub-horizontal and exhibits a geopetal level. (b) Coarsening upward FG microfacies overlying steep topography and one grike filled with FP microfacies. The shaded area shows how the zone affected by iron extend laterally into the FG microfacies, indicating the relative age of the iron-crust. (c) Splitkarren with ArS overlain by FG microfacies, the former with abundant calcite laths. Note internal, laminated, slightly silty peloidal wackestone (lpw) at the base of the grike. (d) AS microfacies hanging on the steep flanks of the siltstone. Note traces of a biogenic laminar crust (blc), frequent 'black grains' in the upper centimetres of the DS microfacies, and the calcite veins originating from small cavities on the lower bedding plane. The encircled numbers in (a) and (b) indicate the positions for the stable isotope values given in Table 1.

ous limestone and to dolomitic siltstone. The most common facies appears to be a mixture of the latter two (Fig. 6a). Mica and feldspar occur only in very small quantities. The total insoluble content (i.e., including silica and iron) by weight of the topmost centimetres of the DS microfacies measures between 20% and 25%, of which almost 90% is in the clay–silt fraction. The average content within the member is generally higher and the facies is herein, for convenience of shortness, referred to as siltstone. Intergrain areas are occupied by micrite, neomorphic microspar and dolomite. The dolomite rhombs are often black under crossed polars, but white with a dark rim in transmitted light. SEM study indicates that the dark rim is an expression of selective leaching of dolomite rhombs, most frequent along the contact, leaving a pitted fabric in the matrix.

5.2. Altered siltstone (AS) (ArS)

The altered siltstone microfacies occurs in two forms; as an in situ but profoundly affected zone (AS) and as a redeposited form (ArS). The AS microfacies occurs at the transition from the siltstone to the oncolite (Figs. 4a and 5d), and as a thin zone along the margins of swallets. In hand-specimens this lithology is light brown with dark spots of iron. In thin section, it is characterised by a clotted micritic texture (occasionally peloidal) mixed in with the siltstone, giving it a diffuse, grey and dull appearance.

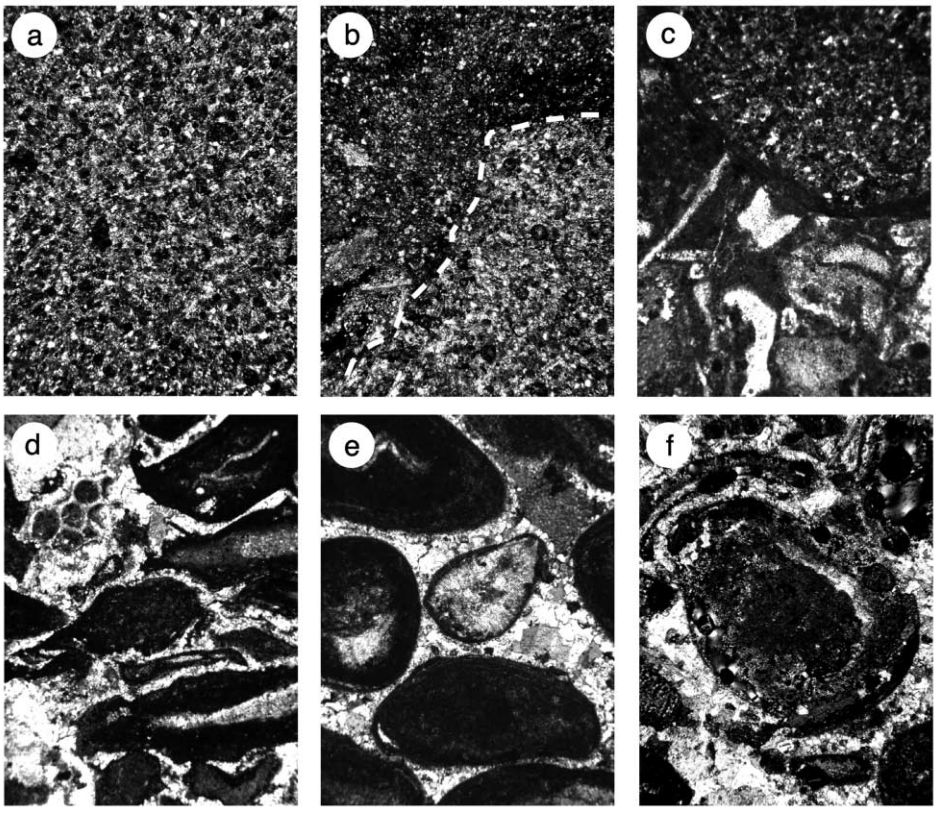

Fig. 6. Micrographs of the different microfacies. All photos 40 ×. (a) Dolomitic siltstone microfacies. (b) Small-scale relief in the dolomitic siltstone (lower right) draped by redeposited siltstone (ArS microfacies). (c) Ferruginous packstone microfacies with one well-rounded and algal-coated siltstone clast. (d) Lower centimetres of the ferruginous grainstone microfacies. Note intense etching on thickly algal-coated allochems and a fitted grain-fabric. (e) Upper part of the ferruginous grainstone microfacies. Note the lack of etching and a more spaced texture as compared to the lower ferruginous grainstone microfacies. (f) Circum-granular cracking in coated grain. Lower ferruginous grainstone microfacies.

The ArS microfacies occurs as infill in grikes and swallets in the upper part of bed 424 and in several places of bed 423 (Figs. 3, 5c and 6b). Compared to the AS microfacies the ArS microfacies is enriched in iron and siltsized quartz. Further, in contrast to the DS and AS microfacies it is generally mixed with both coated and uncoated carbonate allochems of which many show different grades of etching. This mixing together with the texture and the stratigraphic position suggests that the ArS microfacies is the product of erosion and redeposition of the DS microfacies subsequent to the introduction of algae in the environment.

5.3. Ferruginous crinoid algal packstone (FP)

A 2-cm-thick, slightly ferruginous and dense packstone (occasionally wackestone) occupies the lower parts of the scalloped, karstic surface. The skeletal composition is dominated by disarticulated and abraded crinoid and brachiopod grains, and subordinate bivalve, ostracode, bryozoan and trilobite fragments (Fig. 6c). A substantial part of these grains is enclosed by a dense grey, only faintly textured, algal coating of *Girvanella–Wetheredella* type. The coating is generally thin but may be several times thicker than the diameter of the enclosed nucleus. Similar algae also occur in the micritic to microsparitic/partly microdolomitic matrix, giving it a patchy texture. Quartz grains are variously abundant in the matrix and may be incorporated in the coating of carbonate allochems. Therefore, this microfacies is transitional to the ArS microfacies. Secondary porosity (intra- and intergranular) is occupied by drusy calcite spar or silica and, in some cases, intragranular dolomite.

A dense, cream-white variety of this packstone facies occur mostly in the lowest parts of the karst topography (Figs. 4b–c and 5a).

5.4. Ferruginous oncolitic grainstone (FG)

The base of the grainstone facies is sharp and situated within the iron-crust zone. Where the crust is horizontal, it separates the FP and FG microfacies (Figs. 4b–c and 5a) or the ArS and FG microfacies (Fig. 5c, and below). The skeletal composition is similar to that of the FP microfacies, but grains differ in a genetic sense: in the FG microfacies all grains are thickly coated and composite micro-oncoids (ooids?) are common. Crinoid grains strongly dominate as nucleus in coated grains, whereas algae and brachiopods less frequently are the host. A substantial number of the coated grains are micritized. One rounded intraclast of the FP microfacies occurred low in the FG microfacies. There are slight differences between the lowermost and the uppermost FG microfacies (Fig. 6d–e).

The lowermost centimetre of the FG microfacies (e.g., thin section G99-432MC, Fig. 4b) shows an overall fitted grain-fabric, circum-granular cracking (sensu Esteban and Klappa, 1983; Fig. 6f), as well as slight pre-lithification compaction features of single grains. Etching on micro-oncoids is common and is often more intense on the upper surface of the grain.

5.5. Siltstone conglomerate (SC)

The lowermost centimetres of the Bara Oolite Member contain frequent extraformational clasts of the Gannarve Member (Figs. 4a–b and 6c). They occur in three of the microfacies listed above (ArS, FP and FG) and generally have a 1-mm or less thin coating of dense grey algae (*Girvanella–Wetheredella* type). The clasts range in size from coarse sand to gravel (2–25 mm, generally ca. 10 mm) and are always well rounded to sub-rounded. This is a striking difference when compared to the situation at Svalings 1 (Fig. 2) where a coeval rocky shore conglomerate consists of reef-derived, pebble-sized clasts, which have exclusively oblate forms (Calner and Säll, 1999). At Klintebys 1, the coarse sand sized fractions of the conglomerate occur also beneath the topmost karstified bed, i.e., along the lower bedding plane of bed 423. Several siltstone clasts show fissures filled with either sediment (syndepositional) or equant calcite spar. One algal-coated clast was found in the uppermost centimetre of bed 424 indicating erosion and redeposition prior to epikarst formation at the Gannarve–Bara Oolite boundary. The conglomerate also occurs in an algal, peloidal grainstone of the lowermost Bara Oolite Member at Mulde 1, 3500 m towards the southwest, and palaeogeographically more seaward (Figs. 2 and 3). The largest clast from that locality measures 15×10 mm. The contact between the Gannarve Member and the Bara Oolite

Member is conformable at Mulde 1, indicating some seaward transport of the conglomerate.

6. Microscopic features

6.1. Calcite laths

Brooms of calcite laths, in which each lath is ca. 70–100 μm wide and sometimes several 1000 μm long, occur low in the ArS microfacies (Figs. 4d and 5c). The major part of the laths is attached to the walls of the vertical down-cuttings and is coalescensing towards the centre of the (former) cavity (Fig. 7a). Others are attached to gravels, e.g., where the siltstone conglomerate occurs in the ArS microfacies.

6.2. Biogenic structures

Four structures of inferred microbial origin occur in association to the contact, by far most abundantly in the ArS and FP microfacies.

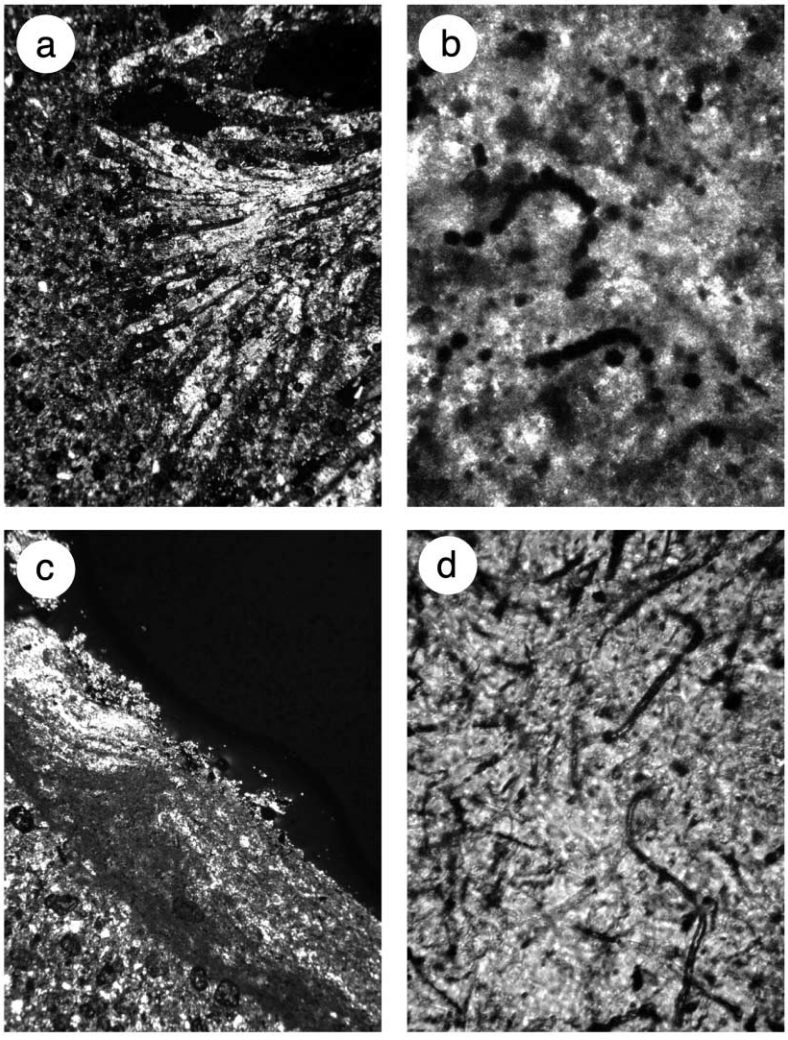

Fig. 7. Micrographs of selected microscopic features. (a) Broom of calcite laths attached to the wall of a sinkhole and growing laterally into the former cavity (40 ×). (b) Filamentous microorganisms preserved as iron oxide in algal coating (400 ×). (c) Biogenic laminar mat encrusting the dolomitic siltstone microfacies (40 ×). (d) Abundant tube-formed filamentous structures preserved on crinoid grain (400 ×).

(1) Elongate structures of dark reddish limonite occur frequently in the cortex of micro-oncoids and within detrital calcite grains. They form slender, curved (worm-like) structures (Fig. 7b), generally somewhat less than 5 μm thick and ca. 50–75 μm long. However, abundant, similar structures in a corroded shell structure measured less than 1 μm in width and about 10 μm in length. Depending on their orientation in the thin-sections they appear as single dots, sub-connected dots ('pearl necklace'), or as sinusoidal threads. In a few places, often on crinoid grains, they occur in crowds radiating from one spot. These structures are similar to others generally interpreted as formed due to fungal/algal activity (see, e.g., Esteban and Klappa, 1983, especially Fig. 76; Di Stefano and Mindszenty, 2000).

(2) In thin section G99-433MC, the AS microfacies is encrusted by a 2–3-mm-thin crust of alternating micritic and microsparitic laminae (Fig. 7c). The crust is partly rich in the reddish limonite structures described above.

(3) Dark grey, straight needle-shaped structures appear as dark lines in one micrite filled boring in a pebble of the siltstone conglomerate. The needles are arranged in a lattice in which single needles cross one another forming a complex mesh. The needles are less than 5 μm in width and about 50–60 μm long. They resemble structures previously referred to as formed by endolithic fungi, e.g., in Pleistocene calcareous crusts (Kahle, 1977, especially Fig. 3c).

(4) Elongate and slightly undulating tube structures, 1–2 μm in width and 50–100 μm long occur frequently on allochems in the FP and lowermost FG microfacies, preferentially on crinoid grains (Fig. 7d).

7. Evidence for a karst origin

Knowledge of the regional geology is crucial to the interpretation of palaeokarst (Esteban and Klappa, 1983). Previous papers on facies analysis and sequence stratigraphy within the Late Wenlock of Gotland is therefore of interest in this discussion (summarised in Fig. 2). The siliciclastic-rich Gannarve Member shoals up from laminated graptolitic mudstones to the herein described unconformity over approximately 5 m. The regression culminated at the closing of the *C. lundgreni* Chron and was eustatic (cf. Loydell, 1998; Calner and Jeppsson, 1999). Throughout a major part of the Baltic basin, the lowstand resulted in a prominent unconformity striking southwest–northeast (the S_4 unconformity of Flodén, 1980). The unconformity at Klintebys 1 is coeval with this major depositional break (Calner and Säll, 1999) and is therefore of regional, rather than local, importance. Towards the northeast, along the strike, the unconformity yields palaeotopography exceeding 5.76 and 16 m of relief at Svalings 1 and Bara 1, respectively (Fig. 2; Calner and Säll, 1999). Further towards the northeast, about 50 km east of Gotland, the dip of the S_4 unconformity is about 12° towards the south sector and is interpreted to become conformable in an area ca. 8.5–10 km south of its appearance (Maria Eriksson, writt. comm. 1999, based on transect 9307 of Flodén, 1980). The unconformity is further traceable into the East Baltic area (Flodén, 1980) where a hiatus occurs at the corresponding stratigraphic level (cf. Nestor and Nestor, 1991). Importantly, the strata southwest of Klintebys 1 are conformable, and thus, Klintebys 1 represents the feather edge of the S_4 unconformity and, thus, the maximum seaward position of the shoreline. This understanding for the regional geology supports that karstic processes formed the unconformity at Klintebys 1. The set of observations at the locality pointing towards subaerial exposure and karstic processes include: (a) erosional relief with undercutting and an associated conglomerate; (b) vertical and subvertical conduits, indicating gravitationally controlled waters; (c) widening of fissures and subsequent polyphase fillings (splitkarren); (d) eluviated, internal sediment (e.g., crystal silt); (e) blackening; (f) repeated etching of carbonate allochems; (g) a fitted grain-fabric; (h) circum-granular cracking; (i) pendant nonluminescent cements; and (j) abundant intercrystalline and intergranular (secondary) porosity. In addition, conodont collections bracketing the unconformity indicate that a *Panderodus unicostatus*-dominated fauna recovered from the topmost 0.04 m of the Gannarve Member at Gannarveskär 4 is lacking at Klintebys 1 (i.e., the lowermost Subzone 2 of the *Ozarkodina bohemica longa* Zone; L. Jeppsson in Calner, 2000). It is therefore likely that at least a few decimetres of the topmost Gannarve Member in the eastern Klintehamn area were eroded during the lowstand. From this discussion, it is evident that the area southwest of

Klintebys 1 is the only one in the Baltic basin where the end-*lundgreni* interval is comformable in outcrop.

Stable isotopes put additional evidence for emersion and karstic processes. Analysis of the $\delta^{13}C$ and $\delta^{18}O$ stable isotopic composition was carried out on the DS, FP and FG microfacies. The isotopic composition changes from one microfacies to another (Fig. 5a–b; Table 1), supporting the conclusion above that these formed in stages separated by some time. It further supports that the karst was formed during the Late Wenlock. A post-Silurian genesis due to interstratal or percolating water-flows would not give rise to the observed microstratigraphy or the changing isotopic composition. The most notable isotopic changes across the contact are a positive shift in the carbon isotope within the FG microfacies and a negative shift in the oxygen isotope within the FP microfacies. The increasing $\delta^{13}C$ values in the FG microfacies could be a response to the high biological activity in that microfacies. However, that clash with an extensive stable isotope data base suggesting that changes in the carbon isotope occurred independent of local facies, and that regional to global factors controlled that curve (Samtleben et al., 2000). The negative $\delta^{18}O$ shift across the contact is interpreted as reflecting increased meteoric influences associated to karstification. With regard to previous stable isotope curves from Gotland, the comparably high isotopic values at Klintebys are consistent with an extremely shallow water depositional environment [the previous curves show a close relationship to depositional depth throughout the succession with distinct positive $\delta^{13}C$ and $\delta^{18}O$ excursions close to but preceding emersion surfaces (Samtleben et al., 1996, 2000)].

Table 1
Stable isotope data from the different microfacies

	d13C PDB	d18O PDB	
Dolomitic siltstone (DS)	1.74	− 5.56	①
	1.72	− 5.47	②
	1.73	− 5.58	③
Ferruginous packstone (FP)	1.40	− 6.52	④
	1.84	− 6.21	⑤
Ferruginous grainstone (FG)	2.87	− 5.08	⑥
	2.68	− 5.11	⑦

Encircled numbers correspond to sample numbers in Fig. 5a–b.

8. Formation of the epikarst

8.1. Erosional phase

The siltstone conglomerate shows that the Gannarve Member was lithified when the erosion started. Where the topmost preserved bed was cut by micro-swallets, gravitational flows resulted in that aggressive waters flowed along the interface to the underlying bed resulting in the upward convex cavities, a few millimetres deep, from the lower bedding plane of bed 423. Later compaction resulted in the spar-filled fractures originating from these zones (Fig. 4c–d). The more fine-grained fractions of the siltstone conglomerate were transported down into the swallets and were trapped in the cavities on the underside of the bed.

The frequent micro-swallets indicate at least a slight, local concentration of the drainage pattern near Klintebys 1, and hence that higher, exposed topography existed nearby. This view is strengthened by the presence of siltstone conglomerate in all microfacies including the altered parent rock (ArS microfacies). In a similar way, this favours the interpretation that the lithified rocks of the Gannarve Member were, in a close vicinity, still exposed for erosional processes at the time of ooid(?) and oncoid formation. Together these observations indicate a ‘karstic flat’ with a probable local relief of a few decimetres. A polyplacophoran mollusc biota inhabited this rocky coast, indicating an upper littoral to intertidal setting (Cherns, 1999). However, no in situ rocky shore community has yet been recovered from Klintebys 1. Absence of clinging or encrusting organisms and the scarcity of borings may be due to transgressive erosion of the surface (cf. Cherns, 1982).

A major control on the amplitude of karst topography and the extent of subsurface karst is the permeability of the parent rock including the availability of fractures or similar conduits, and the mineralogical phase of $CaCO_3$; dolomites are several orders of magnitude less soluble than limestones in meteoric water (Choquette and James, 1988). As the Gannarve Member contains a substantial amount of siliciclastic material in a matrix with abundant dolomite, and since the unit was entirely lithified prior to erosion, the permeability was inferably very low. Therefore, the Gannarve Member probably transmit-

ted groundwater mainly by conduit flow. Although larger excavations and areas need to be studied, it is likely that these were the main factors limiting the relief of the epikarst at Klintebys 1. Another important factor may have been a short period of exposure. The distal position of the Klintebys 1 locality along the S_4 unconformity and the preservation of coeval palaeotopography in more proximal settings supports this rapidity.

8.2. Depositional phase

As indicated above, the Bara Oolite Member was deposited along a rocky coast, although with varying topography, both on eastern and on western Gotland. The different microfacies, the diagenetic sequence, and the repeated occurrence of (petrographically different) well-rounded intraclasts, and erosional contacts (including the satellite iron-crusts) in the overlying 2 dm of the algal grainstone, indicate that initial deposition of the Bara Oolite Member was rhythmic with several periods of etching and/or non-deposition.

The observations that the siltstone conglomerate became rounded prior to algal coating and that the coating is thin may indicate a 'late entrance' of algae, and that they were important encrusters only along the transgressive shores, but not along the lowstand coast. This is further supported by the rarity of algal lining along the karstic topography (only two records), and the contrastingly very thick coating on many clasts of the basal TST (FP and FG microfacies).

The lower parts of the FP microfacies is rich in whitish micrite and inferred filamentous microorganisms. The presence of one rounded clast of the FP microfacies in the overlying FG microfacies indicate that this early transgressive deposit was at least semi-lithified before the FG microfacies was deposited.

The lateral extension of iron (Fig. 5b) into the topmost DS and basal FG microfacies clearly shows that this zone was not related to the formation of epikarst, but that it formed *after* the deposition and first dissolution of the FG microfacies (cf. similar principal results of Di Stefano and Mindszenty, 2000), but prior to its lithification. Consequently, the zone formed synsedimentary at least a few centimetres below the sediment surface and does not alone indicate subaerial exposure or karstification. Within this zone and in the first few millimetres above it, circumgranular cracking of coated grains is common. Such structures form through repeated wetting and drying, generally landward of the intertidal area (Esteban and Klappa, 1983, and references therein). At Klintebys 1, such a situation could be due to repeated evaporation of meteoric water transported to the lithified flat.

Since the highest rate of microbial activity correlates with the vertical range of the iron zone, reducing conditions may have prevailed. Since the iron-zone is geopetal in origin, it may be an expression related to the groundwater-table. A capillary level is less likely since the permeability in unlithified grainstone is likely to have been very high. The possible areal extent of the iron-crust over many thousands of square metres (see Section 2) strengthens the interpretation that the topographical relief was small in the Klintehamn area.

9. Diagenesis of the transgressive systems tract

9.1. Diagenetic features

Cathodoluminescence indicates two early (but post-dating the formation of the iron zone) generations of calcite cement in the transgressive grainstone facies. These two generations were subsequently partly dissolved by aggressive waters, and succeeded by a third calcite cement generation and silicification. The silicification may be attributed to the close stratigraphical presence of the Grötlingbo Bentonite, which was deposited across the basin during the *Pristiograptus dubius parvus* Zone (cf. Laufeld and Jeppsson, 1976; papers in Calner, 2000).

The basal FG microfacies (e.g., thin section G99-432MC) shows intense etching on allochems. Uninterrupted, thin isopachous rims lining corroded allochem surfaces show that the first stage of etching occurred in the unlithified bioclastic sands. Some grains show three stages of dissolution; on the grain itself, after the first coating, and after a second period of algal encrustation. This indicates alternating marine and fresh-water conditions, typical for the intertidal area. The trend of repeated dissolution resulted in a fitted grain-fabric, i.a., an intergranular chemical compaction (Fig. 6d). The first cement generation is nonluminescent, generally isopachus, but sometimes

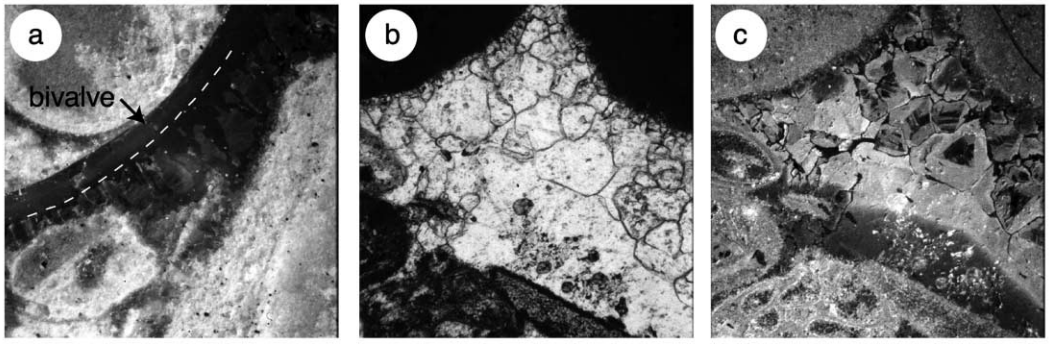

Fig. 8. SEM and CL micrographs from the karst unconformity. (a) Nonluminescent bivalve shell with dull first generation cement from the basal Bara Oolite Member at Klintebys 1 (G99-432MC). (b) Micritized coated grains with a thin first generation cement and a succeeding drusy porefilling cement, from the topmost Bara Oolite Member at Klintebys 1. (c) Approximately the same view as in (b) under CL. Note the contrastingly dull first generation around coated grains and in the intergranular porosity of the bryozoan grain (br). Note also how calcite crystals 'float' on a black background (silica). All photographs approximately 2 mm across.

better developed below grains (Fig. 8a). The second cement generation was a drusy or syntaxial intergranular spar that occluded the remaining porosity. As is the case on grains, also cements are truncated. The second generation spar crystals are truncated by the satellite iron-crusts. Intragranular silica is common.

The topmost FG microfacies (bed G96-83MC) does not show any fitted fabric. Instead, a 'spaced' texture indicates rapid lithification (Fig. 6e), and decreased availability of meteoric waters, possibly due to continued transgression. Grains often constitute a patchy isopachous rim of very fine-grained, 'sugar-textured', equant spar (equicrystalline texture) which is contrastingly dark in CL (Fig. 8b–c). This early cement sometimes form a meniscus at grain contacts, however, these are dull coloured in CL. Primary intergrain pore space is occluded by syntaxial calcite (where crinoid grains occur) or by drusy spar. These crystals are dull in CL and show abundant micro-etching (cf. Meyers, 1988, fig. 14.7A) at crystal boundaries. The core of the crystals is dark with a very thin concentric zonal banding in CL, indicating that pore-water chemistry changed during shallow burial. This is the case also for intragranular drusy spar. The resulting intercrystalline secondary porosity is partly occluded by a silica cement (Fig. 8b–c).

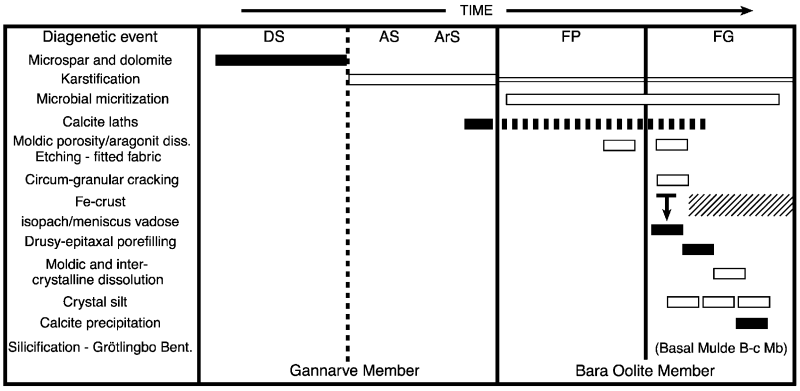

Fig. 9. Summary of diagenetic events and their timing across the epikarst at Klintebys 1, starting with the lithification of the Gannarve Member. Black rectangles indicate cement phases, whereas open ones indicate creation of secondary porosity. Downward pointing arrows indicate stages of compaction.

Crystal silt (Dunham, 1969) occurs both as intragranular geopetals and in intergranular areas. The relative timing of diagenetic events is shown in Fig. 9.

10. Conclusion

(1) Small-scale topography, solution features (kamenitzas, grikes, sinkholes), biogenic structures, Fe-encrustations and an extraformational conglomerate at the Middle Silurian Fröjel–Halla formational boundary on Gotland is interpreted as epikarst.

(2) Four microfacies are associated to the epikarst: Regressive dolomitic siltstone and altered siltstone occur below the contact, forming the topmost Fröjel Formation, and represent the unaffected and affected parent rock, respectively. Ferruginous crinoid algal packstone and ferruginous oncolitic grainstone occur above the contact, representing a condensed transgressive lag facies belonging to the basal Halla Formation.

(3) Microstratigraphical relationships show that a thin but laterally extensive Fe-crust at the contact was not directly related to subaerial exposure but is a synsedimentary geopetal that formed a few centimetres below the sea-floor during the ensuing transgression.

(4) The diagenetic sequence and fabrics of the basal transgressive cover indicate that it experienced several stages of fresh-water dissolution in the vadose percolation zone, viz. (a) truncation of early cements, (b) etching of grains, often most extensive on the upper grain surface, (c) a fitted grain-fabric, (d) pendant cements, (e) internal sediments: e.g., crystal silt, and two type of eluviated microfacies, and (f) intercrystalline (secondary) porosity.

(5) Stratigraphic repetition of conglomerates and marine and meteric influences to the studied succession, as well as local and regional facies, suggest that the epikarst formed in a lowstand intertidal setting.

(6) The epikarst represents the feather edge of a basin regional unconformity and, thus, the maximum seaward position of the Baltic Basin shoreline during the end-lundgreni global lowstand. It is associated to previously reported global extinctions among graptolites, conodonts and chitinozoans. This paper therefore shows that the unconform transition is of global rather than, as previously thought, local importance.

Acknowledgements

Lennart Jeppsson, Anders Ahlberg, Hanna Calner (all at Lund University), Axel Munnecke (Tübingen University), and Lesley Cherns (Cardiff University) are acknowledged for their constructive comments on this manuscript. I am grateful to Paul Wright (Cardiff University) who shared unpublished data, took time to study parts of the material at an early stage and contributed with useful pieces of advice. Noel P. James and one anonymous referee improved the manuscript with their own pieces of advice. The Royal Physiographical Society of Lund financed the study of stable isotopes. The Division of Historical Geology and Palaeontology, Lund University, financed additional laboratory costs and also provided working facilities.

References

Baceta, J.I., Wright, V.P., Pujalte, V., in press. Palaeo-mixing zone karst features from Palaeocene carbonates of north Spain: first ancient example of widespread diagenetic system. ExpresSed. Sedimentology.

Calner, M., 1999. Stratigraphy, facies development, and depositional dynamics of the Late Wenlock Fröjel Formation, Gotland, Sweden. GFF 121, 13–24.

Calner, M., 2000. Stratigraphy and facies of Middle Silurian epicontinental carbonate platform deposits of Gotland, Sweden. Lund Publ. in Geol. 150, pp. 1–18 [Unpublished thesis].

Calner, M., Jeppsson, L., 1999. Emersion and subaerial exposure in the Silurian of Gotland—response to a mid-Homerian glaciation. GFF 121, 78–79.

Calner, M., Säll, E., 1999. Transgressive oolites onlapping a Silurian rocky shoreline unconformity, Gotland, Sweden. GFF 121, 91–100.

Calner, M., Sandström, S., Mõtus, A.-M., 2000. Significance of a Halysitid-Heliolitid mud-faces auotobiostrome from the Middle Silurian of Gotland, Sweden. Palaios 15, 511–523.

Cherns, L., 1982. Palaeokarst, tidal erosion surfaces and stromatolites in the Silurian Eke Formation of Gotland, Sweden. Sedimentology 29, 819–833.

Cherns, L., 1999. Silurian Chitons as indicators of rocky shores and lowstand on Gotland, Sweden. Palaios 14, 172–179.

Choquette, P.W., James, N.P., 1988. Introduction. In: James, N.P., Choquette, P.W. (Eds.), Paleokarst. Springer-Verlag, New York, pp. 1–21.

Di Stefano, P., Mindszenty, A., 2000. Fe–Mn-encrusted "Kamenitza" and associated features in the Jurassic of Monte Kumeta (Sicily): subaerial and/or submarine dissolution? Sediment. Geol. 132, 37–68.

Dunham, R.J., 1969. Early vadose silt in the Townsend Mound

(reef), New Mexico. In: Friedman, G.M. (Ed.), Depositional Environments in Carbonate Rocks (a Symposium). Soc. Econ. Paleontol. Mineral., Spec. Publ., vol. 14, 139–181.

Esteban, M., Klappa, C.F., 1983. Subaerial exposure environment. In: Scholle, P.A., Bebout, D.G., Moore, C.H. (Eds.), Carbonate Depositional Environments. Am. Assoc. Pet. Geol. Mem., vol. 33, 1–54.

Flodén, T., 1980. Seismic stratigraphy and bedrock geology of the central Baltic. Stockholm Contributions in Geology 35, 1–240.

Hadding, A., 1929. The Paleozoic and Mesozoic sandstones of Sweden. The pre-Quaternary sedimentary rocks of Sweden III. Med. Lunds Geol.-Min. Inst. 41, 287 pp.

Hede, J.E., 1921. Gottlands silurstratigrafi. Sv. Geol. Undersök. C 305, 1–100.

Hede, J.E., 1927. Berggrunden (Silursystemet). In: Munthe, H., Hede, J.E., Lundquist, G. (Eds.), Beskrivning till kartbladet Klintehamn. Sv. Geol. Undersök. Aa, vol. 160, 12–48.

Hede, J.E., 1960. The silurian of gotland. In: Regnéll, G., Hede, J.E. (Eds.), The Lower Palaeozoic of Scania. The Silurian of Gotland. Guide to excursions A22 and C17, 21st International Geological Congress, Norden, 44–89.

Jaeger, H., 1991. New standard graptolite zonal sequence after the "big crisis" at the Wenlockian/Ludlowian boundary (Silurian). N. Jb. Geol. Paläontol., Abh. 182, 303–354.

Jeppsson, L., 1997. Recognition of a probable secundo-primo event in the Early Silurian. Lethaia 29, 311–315.

Jeppsson, L., 1998. Silurian oceanic events: a summary of general characteristics. In: Landing, E., Johnson, M.E. (Eds.), Silurian cycles: linkages of dynamic stratigraphy with atmospheric, oceanic and tectonic changes. James Hall Centennial Volume. N.Y. St. Mus. Bull. vol. 491. The University of the State of New York, The State Education Department, pp. 239–257.

Kahle, C.F., 1977. Origin of subaerial Holocene calcareous crusts: role of algae, fungi and sparmicritisation. Sedimentology 24, 413–435.

Kahle, C.F., 1988. Surface and subsurface paleokarst, Silurian Lockport, and Peebles Dolomites, western Ohio. In: James, N.P., Choquette, P.W. (Ed.), Paleokarst. Springer-Verlag, New York, pp. 229–255.

Kaljo, D., Boucot, A.J., Corfield, R.M., Le Herisse, A., Koren, T.N., Kriz, J., Männik, P., Märss, T., Nestor, V., Shaver, R.H., Siveter, R.H., Derek, J., Viira, V., 1995. Silurian bio-events. In: Walliser, O.H. (Ed.), Global Events and Event Stratigraphy in the Phanerozoic. Springer-Verlag, New York, pp. 173–224.

Kluessendorf, J., Mikulic, D.G., 1996. An early silurian sequence boundary in Illinois and Wisconsin. In: Witzke, B.J., Ludvigson, G.A., Day, J. (Eds.), Paleozoic Sequence Stratigraphy: Views from the North American Craton. Geol. Soc. Am., Spec. Pap., vol. 306, 177–185.

Koren', T.N., 1991. The *lundgreni* extinction event in central Asia and its bearing on graptolite biochronology within the Homerian. Proc. Est. Acad. Sci. 40, 74–78.

Laufeld, S., Jeppsson, L., 1976. Silicification and bentonites in the Silurian of Gotland. Geol. Fören. Stockholm Förh. 98, 31–44.

Loydell, D.K., 1998. Early Silurian sea-level changes. Geol. Mag. 135, 447–471.

Meyers, W.J., 1988. Paleokarstic features in Mississippian limestones, New Mexico. In: James, N.P., Choquette, P.W. (Eds.), Paleokarst. Springer-Verlag, New York, pp. 306–328.

Munthe, H., 1915. Oolit med kraftiga böljeslagsmärken vid Klintebys på Gotland. Geol. Fören. Stockholm. Förh. 37, 430–434.

Nestor, V., Nestor, H., 1991. Dating of the Wenlock carbonate sequences in Estonia and stratigraphic breaks. Proc. Est. Acad. Sci. Geol. 40, 50–60.

Samtleben, C., Munnecke, A., Bickert, T., Pätzold, J., 1996. The Silurian of Gotland (Sweden): facies interpretation based on stable isotopes in brachiopod shells. Geol. Rundsch. 85, 278–292.

Samtleben, C., Munnecke, A., Bickert, T., 2000. Development of facies and C/O-isotopes in transects through the Ludlow of Gotland: evidence for global and local influences on a shallow-marine environment. Facies 43, 1–38.

Sivhed, U., 1976. Sedimentological studies of the Wenlockian Slite Siltstone on Gotland. Geol. Fören. Stockholm Förh. 98, 59–64.